LETTERS IN BIOMATHEMATICS
An International Journal

RESEARCH ARTICLE OPEN ACCESS

Stability, Bifurcation and Chaotic Dynamics Analysis of a Discrete-Time Predator–Prey Model with Exponential Growth and Saturated Predation

Dheerendra Kumar[1], Benukar Mondal[2*]

[1]Department of Mathematics, B N Mandal University, Madhepura-852113, Bihar, India
Email: dkdinkar96@gmail.com
[2]Department of Mathematics, Lalit Narayan Mishra Smarak College, Birpur, Supaul-854340, Bihar, India.
Email: benukar.math@gmail.com

ABSTRACT

Discrete population maps can generate complex oscillations even with only two interacting species. This study explores equilibrium stability, bifurcation, and chaotic behavior of a positivity-preserving predator-prey map, including Ricker-type exponential prey growth and a Holling type-II predation response. Stated conditions and the Jacobian allow determination of Jury inequalities and a threshold of the growth rate for loss of coexistence stability. Rather than interpreting numerical results based on field data, we calculate numerical trajectories, bifurcation diagrams, phase portraits, and descriptive statistics, and determine the Lyapunov exponents and other map-related invariants, directly from the map equations. For our illustrative parameter set, coexistence loses stability at r = 3.5361, and at r = 3.8, the behavior is described by a periodic orbit of period two. The largest positive Lyapunov exponent is 0.39 at r = 4.7. A different mortality sweep identifies a crossing of the unit circle on the complex plane, consistent with a Neimark-Sacker bifurcation. Our results provide insight on how various parameters, response functions, and ecological assumptions affect the dynamics of predator-prey systems, and remain ecologically conditioned on calibration to field data..

ARTICLE HISTORY
Received October 15, 2026
Accepted November 19, 2026

KEYWORDS
Predator–prey model; discrete-time dynamics; local stability; bifurcation; chaos

1. Introduction

Predator-prey interactions couple consumer demand to resource supply. Difference equations can describe recruitment and mortality more adequately than continuous equations when generations are non-overlapping or populations are monitored seasonally. Such equations can generate fixed points, limit cycles, invariant curves, and sensitive dependence on initial conditions. Research on discrete predator-prey systems have documented these behaviors under assumptions of satiated feeding, the presence of refuges, or predator harvesting (Al-Basyouni & Khan, 2020; Santra et al., 2021; Arias et al., 2022).

A density-dependent Ricker-type recruitment reduces the abundance of a prey species by an exponential factor. Positivity of the associated exponential map presents biological interpretability. However, predator growth can become strongly overcompensatory at high intrinsic rates. Diminishing marginal consumption can be modeled by a Holling type-II function. Studies on Ricker dynamics, carrying capacity, and non-linear saturation motivated an integrated analytical-numerical approach (Rajni & Ghosh, 2022; Hamada et al., 2023; Seralan et al., 2023).

This study focuses on an exponential map and determines equilibrium conditions as well as the stability of the equilibrium. The study locates the flip threshold, and in a second parameter sweep, identifies a possible Neimark–Sacker bifurcation. Lastly, the study distinguishes chaos from periodic orbits by computing the first two Lyapunov exponents. The goal of the study is to provide a case analysis on the specific exponential map rather than broadly generalize on the basis of limited ecological data.

CONTACT Benukar Mondal: benukar.math@gmail.com

2. Review of Literature

Arias et al. (2022) established bifurcation and chaotic scenarios for a discrete model with Holling-II feeding, while Rajni and Ghosh (2022) identified multistability and changes in mean densities in a discrete Rosenzweig–MacArthur model. Hong and Zhang (2023) studied a Neimark–Sacker bifurcation in a model with prey refuge. Singh and Sharma (2023) analyzed flip, transcritical and Neimark-Sacker bifurcations and chaos control. Chaos in the coupled logistic map is reported in Al-Kaff et al. (2024). Ruan and Li (2024) analyzed Leslie-Gower dynamics in a semi-discrete case. Chen and Li (2024) studied ratio-dependent bifurcations. Liu et al. (2024), and Lv and Li (2024) reported higher-codimension phenomena. Spatial effects of refuge and alternate Holling responses offer new behavioral possibilities (Zhang et al., 2024; Khan and Uddin, 2025; Liu et al., 2025). In Holling-II systems, Mehdi et al. (2025) report on stability and chaos and utilize Lyapunov exponents. These works provide motivation to consider each threshold for the particular exponential map, and not ape results for incompatible models.

Mathematical Model and Methodology

3. Model formulation

Let x_t and y_t denote prey and predator abundances. The following Ricker–Holling-II difference equations define the system, with all parameters strictly positive.

$$x_{t+1} = x_t \exp\left[r\left(1 - \frac{x_t}{K}\right) - \frac{ay_t}{1 + hx_t}\right]$$

$$y_{t+1} = y_t \exp\left[\frac{cax_t}{1 + hx_t} - m\right]$$

r = prey intrinsic growth, K = carrying capacity, a = predation coefficient, h = saturation parameter, c = conversion factor, m = predator mortality. The logarithmic growth terms are A

= r (1 - x/K) - a y/(1 + hx) and B = cax/(1 + hx) - m. Positivity is achieved with respect to the initial conditions because the multipliers are exponentials. The feeding flux, ax/(1 + hx), saturates at a/h. The parameter values are mathematically chosen test values rather than field estimates; only the conceptual modelling framework is literature-informed (Seralan et al., 2023; Hamada et al., 2023).

The equations may also be interpreted as integrating per-capita rates, constant between the sampling occasions. Prey recruitment and predator mortality are influences in a time step. Predation, a removal process, and mortality are influenced by the starting density of the prey population and the starting density of the predator population respectively. It is assumed that during a time step, the prey and predator populations have no other interactions and that the population is homogenous. The map is deterministic, autonomous and spatially homogeneous.

Equilibrium points

Solving $x_{t+1} = x_t$ and $y_{t+1} = y_t$ gives the extinction equilibrium, predator-free equilibrium and potential coexistence equilibrium

$$E_0 = (0,0), \quad E_K = (K, 0), \quad E_* = (x_*, y_*)$$

$$x_* = \frac{m}{ca - mh}, \quad y_* = \frac{r}{a}\left(1 - \frac{x_*}{K}\right)(1 + hx_*)$$

Positive coexistence requires ca > mh and 0 < x* < K, equivalently caK/(1 + hK) > m. At extinction the eigenvalues are e^r and e^{-m}, making the origin a saddle. At (K, 0), they are 1 − r and exp[caK/(1 + hK) − m]; invasion by a rare predator is possible precisely when the second exceeds one.

Linear stability and bifurcation criteria

For f = xe^A and g = ye^B, differentiation gives the Jacobian

$$J(x,y) = \begin{pmatrix} e^{A}(1 + x[-r/K + ahy/(1+hx)^2]) & -axe^{A}/(1+hx) \\ caye^{B}/(1+hx)^2 & e^{B} \end{pmatrix}$$

Write T = tr(J*) and D = det(J*) at the positive equilibrium. Both eigenvalues lie inside the unit disk when the strict Jury conditions hold:

$1 - T + D > 0, \quad 1 + T + D > 0, \quad 1 - D > 0$(6)

The equilibrium identities simplify the trace and determinant to:

$$T = 2 + rL, \quad D = 1 + r(L + C)$$

$$L = x_* \left[\frac{1}{K}, \frac{h(1 - x_*/K)}{1 + hx_*} - \frac{cax_*(1 - x_*/K)}{(1 + hx_*)^2} \right]$$

The first Jury expression becomes rC > 0. The second is 4 + r(2L + C), and the third equals −r(L + C). A flip candidate arises when one multiplier reaches −1, provided the companion multiplier does not also lie on the unit circle, the crossing is transversal, and the necessary nonlinear normal-form coefficient is nonzero. A Neimark–Sacker candidate instead requires a complex pair crossing modulus one, plus nonresonance and nonlinear nondegeneracy (Arias et al., 2022; Hong & Zhang, 2023).

At coexistence, the characteristic polynomial is $\lambda^2 - T\lambda + D$. Its Jury conditions give three separate tests: one ensures the product of eigenvalues remains below the unit threshold, while another detects a multiplier reaching −1. Along the principal r-sweep, L + C is fixed and negative; hence D decreases monotonically as growth increases, so D = 1 cannot provide a Neimark–Sacker threshold for positive r. This is why mortality is selected for the complementary complex-eigenvalue sweep. Eigenvalue calculations characterise local behaviour only and do not exclude distant coexisting attractors.

Numerical procedures

Trajectories use $x_0 = 0.70$ and $y_0 = 0.25$ for the principal sweep, r ranging from 2.75 to 4.78, and fixed K = a = 1, h = 0.1, c = 0.5 and m = 0.3. Each bifurcation point uses 4,100 iterations; the final 85 values are plotted after transient removal. Summary statistics and regime-specific exponents use 14,000 iterations, discarding the first 4,000. The exponent sums logarithmic tangent-vector stretch factors with unit-vector renormalization

$$\lambda_{\max} = \lim_{n\to\infty} \frac{1}{n} \sum_{t=1}^{n} \log \frac{\| v_t \|}{\| v_t \|}$$

A separate sweep sets K = a = 1, h = 0.3, c = 2.3 and r = 1.5 while varying m. Computations use 64-bit floating point arithmetic; sample standard deviations are reported as population

standard deviations of post-transient states. A positive exponent together with a bounded, irregular orbit is treated as numerical evidence of chaos, not a proof of a chaotic invariant set.

The growth sweep uses 740 evenly spaced parameter values for each population bifurcation diagram and 400 values for a Lyapunov plot. The state is reset for each parameter rather than continued from the previous simulation in order to maintain consistency for comparison under a defined starting state. For the exponents, 6,500 iterations are run, with the first 3,500 iterations discarded; the regime summary exponents, however, use the longer 14,000-step procedure. Approximate numerical exponents are highly dependent on the length of the observation, especially for values near zero, and therefore, should be considered in conjunction with phase portraits and repeated verifications of initial conditions. A apparently smooth, quasiperiodic, limit cycle in a finite projection does, however, provide evidence for the presence of quasiperiodic behavior.

Results and Data Analysis

4. Parameter and equilibrium analysis

Table 1. Model parameters used for the principal numerical analysis.

Parameter	Biological interpretation	Value	Basis
r	Intrinsic prey growth	2.75–4.78	Exploratory sweep
K	Prey carrying capacity	1.00	Normalized illustrative value
a	Predation coefficient	1.00	Illustrative value
h	Predation saturation	0.10	Illustrative value
c	Predator conversion	0.50	Illustrative value
m	Predator mortality	0.30	Illustrative value
(x_0, y_0)	Positive initial abundances	(0.70, 0.25)	Numerical initial condition

For this parameter set, x* = 0.638298 and y* = 0.3847895r. The coefficients L = −0.616596 and C = 0.102000 imply L + C < 0. Setting 4 + r(2L + C) = 0 gives the analytical flip multiplier-crossing threshold

$$r_{\text{flip}} = -\frac{4}{2L + C} \approx 3.5360945$$

At r = 3.5361 the second eigenvalue is approximately 0.82, inside the unit circle, and d(1 + T + D)/dr = 2L + C ≈ −1.1312 is nonzero. The numerical diagram displays a nearby stable period-two branch. These checks establish a simple transversal eigenvalue crossing; a formal nonzero cubic flip normal-form coefficient is not evaluated here.

Table 2. Equilibrium points, eigenvalues and local classification at r = 3.0.

Equilibrium	(x, y)	Jacobian eigenvalues	Classification
Extinction E_0	(0, 0)	20.08554; 0.74082	Saddle
Predator-free E_k	(1, 0)	−2.00000; 1.16714	Unstable
Coexistence E*	(0.63830, 1.15437)	0.81634; −0.66613	Locally stable

Statistical dynamics and bifurcation diagrams

Table 3. Post-transient statistics for three population regimes (10,000 iterations retained).

r; regime	Prey: mean ± SD	Predator: mean ± SD	Prey / predator CV	λmax
3.0; stable	0.6383 ± 0.0000	1.1544 ± 0.0000	0.000 / 0.000	−0.2029
3.8; period 2	0.6478 ± 0.3188	1.4206 ± 0.0998	0.492 / 0.070	−0.1079
4.7; chaotic	0.6639 ± 0.5277	1.6714 ± 0.2278	0.795 / 0.136	+0.3933

At r = 3.8, the orbit alternates between prey states near 0.3290 and 0.9667, with corresponding predator states near 1.3208 and 1.5204. At r = 4.7, prey spans 0.0034–2.1740 and predators 1.1307–2.1254 in the retained simulation. The prey can exceed K transiently because K is an equilibrium scale, not a hard cap in an overcompensatory discrete map. Figures 1 and 2 depict the widening orbital branches as r increases.

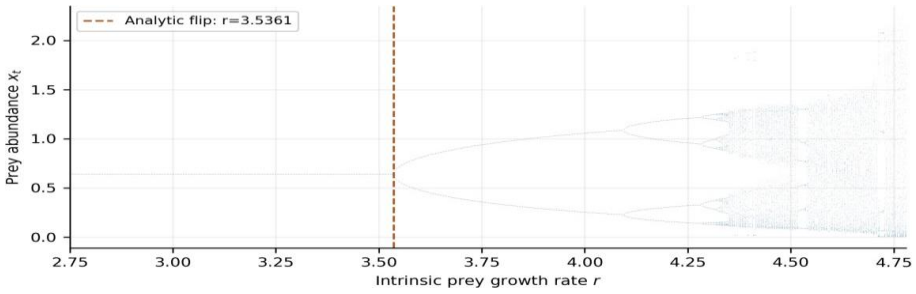

Figure 1. Bifurcation diagram for prey abundance under the intrinsic growth-rate sweep.

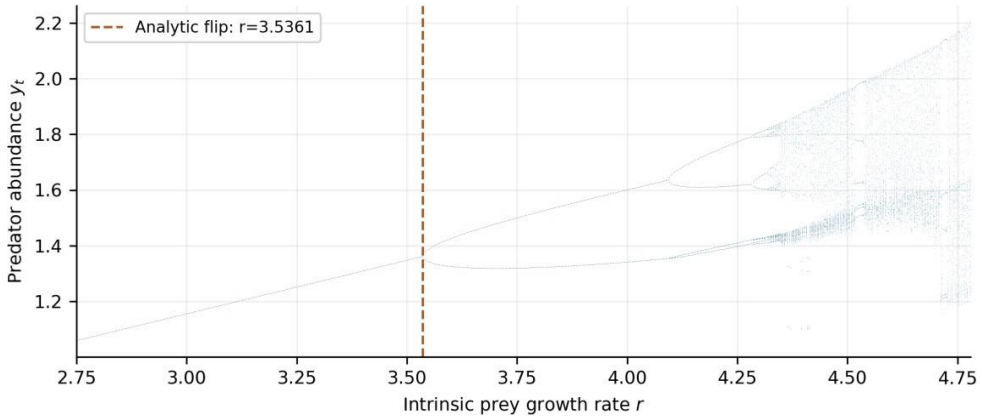

Figure 2. Bifurcation diagram for predator abundance using the same parameter sweep

The descriptive measures reveal why equilibrium-based summaries can be misleading after bifurcation. Mean prey abundance rises only slightly from the stable to period-two regime, but its coefficient of variation increases from zero to approximately 0.492. In the chaotic case the coefficient rises to approximately 0.795, despite positive average prey and predator densities. The minimum prey value at r = 4.7 is especially small, indicating potentially substantial demographic vulnerability if finite-population extinction thresholds were added. Such thresholds are absent from this idealised map, so observed low numerical abundance should not be described as documented extinction.

Phase portraits, time series and Lyapunov diagnostics

The largest Lyapunov exponent is negative at the fixed point (−0.2029) and the stable period-two state (−0.1079), but positive at r = 4.7 (+0.3933). The phase portraits and time series reveal irregular oscillation at r = 4.7 with predators remaining positive throughout the retained window. Positivity and a positive finite-time exponent support sensitive dynamics; neither guarantees persistence for all future times.

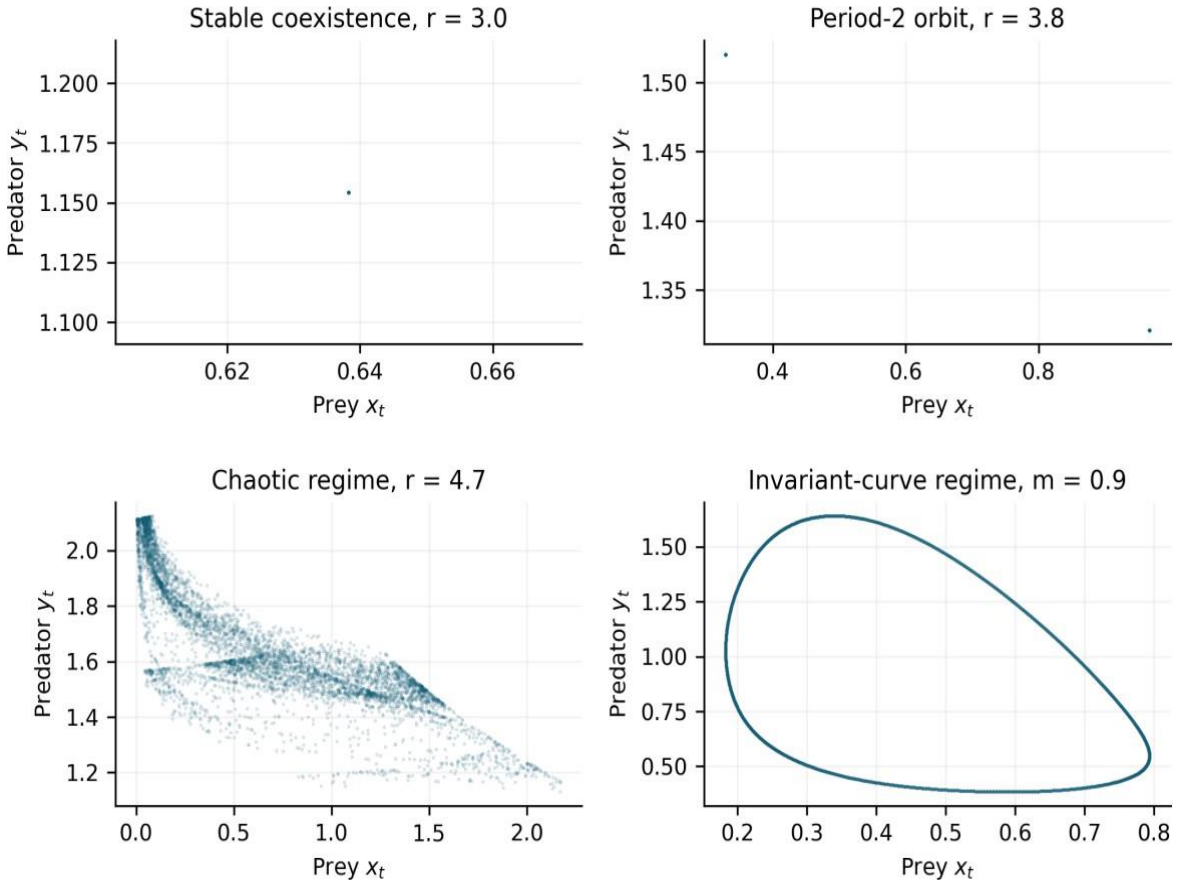

Figure 3. **Principal stable, periodic and chaotic phase portraits; lower-right panel uses the separate mortality-sweep parameter set.**

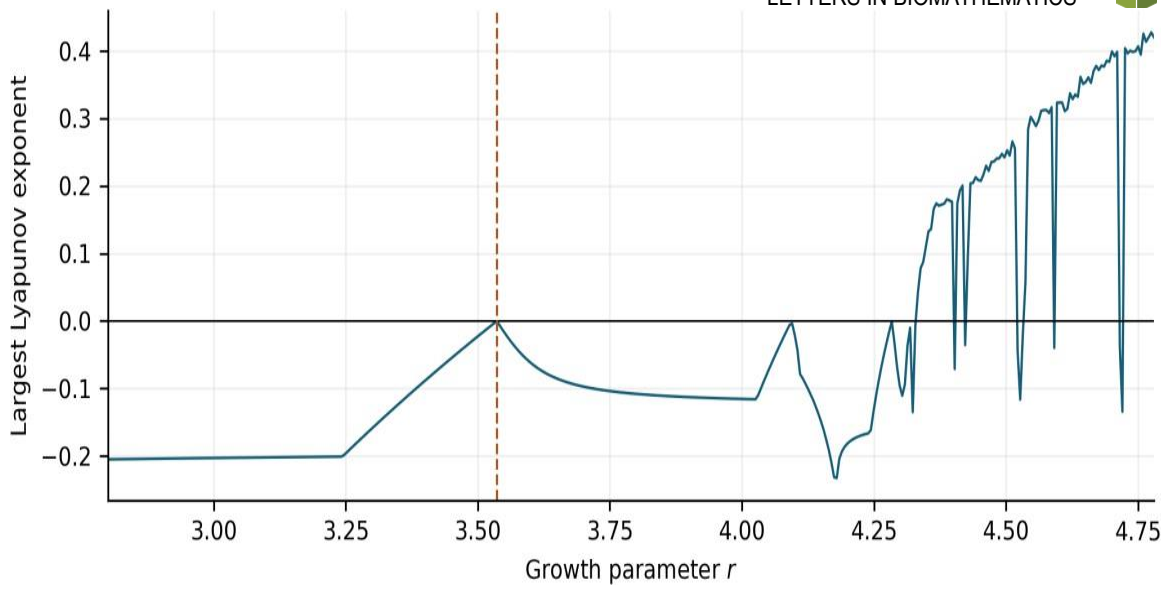

Figure 4. Largest Lyapunov exponent across the principal growth-rate parameter sweep.

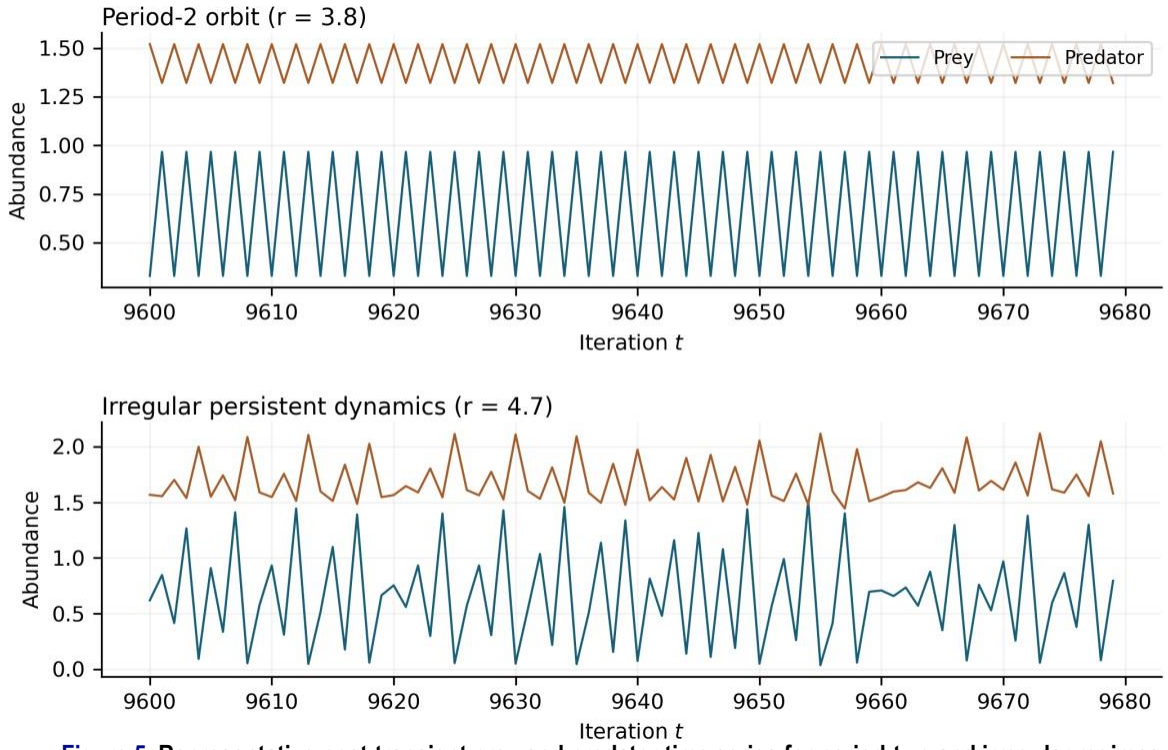

Figure 5. Representative post-transient prey and predator time series for period-two and irregular regimes.

Neimark–Sacker crossing and sensitivity

For the second parameter set, the coexistence equilibrium has complex eigenvalues at m = 1.000: 0.673913 ± 0.738811i, with T = 1.347826 and D = 1. The determinant crosses one transversally as mortality increases, with dD/dm ≈ −1.07283. Hence the necessary linear conditions for a Neimark–Sacker transition hold

$$D(m_c) = 1, \quad -2 < T(m_c) < 2, \quad \left.\frac{dD}{dm}\right|_{m_c} \neq 0$$

For m = 0.9 the equilibrium determinant is 1.0963 and the numerical orbit approaches an apparent invariant curve (largest exponent approximately zero); for m = 1.1, D = 0.8816 and the equilibrium is attracting (largest exponent −0.0631). The first Lyapunov normal-form coefficient is not computed, so the nonlinear bifurcation direction remains a qualified numerical interpretation.

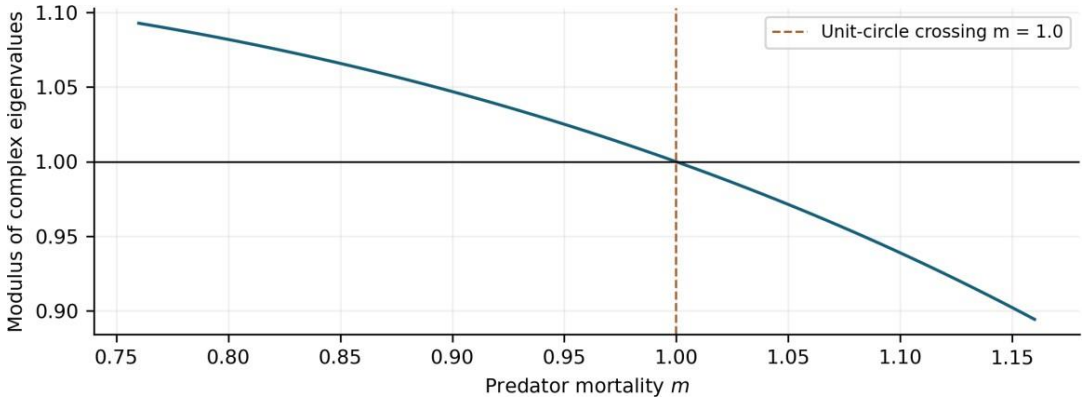

Figure 6. Complex-multiplier modulus and the candidate Neimark–Sacker threshold as mortality varies. Preliminary

condition testing at r = 4.4 showed both positive and negative exponents (−0.2270 and +0.1753 respectively). As r increased to 4.7, three tested initial conditions yielded positive exponents (+0.3896 to +0.3933). At +0.3933, lowering h from 0.10 to 0.07 yielded an exponent of +0.320, while increasing h to 0.13 gave an exponent of +0.508. The existence of positive Lyapunov exponents suggests that high growth can lead to chaotic behavior. Alternatively, low growth can also yield the same. Trajectory sensitivity provides evidence against regarding the behaviors of a single trajectory as universal.

5. Discussion

The analytical and numerical findings predict two local paths departing from coexistence. Under the leading growth-rate sweep, the Jury inequalities predict a fixed-point loss at r ≈ 3.5361, where an eigenvalue crosses −1. The period-two branch is in agreement with a flip bifurcation. High or unbounded growth can produce irregular, bounded fluctuations, and positive Lyapunov exponents, as observed in this study. Similar behaviors are observed in the discrete models of Al-Basyouni and Khan (2020), Arias et al. (2022), Hamada et al. (2023), and Mehdi et al. (2025) although their equations and critical values may differ

The separate mortality sweep demonstrated how it is erroneous to presume all parameters elicit the same bifurcations. A pair of complex conjugate multipliers reaches unit modulus at m = 1, and the computed phase portraits support the presence of an invariant closed curve. Similar mechanisms of Neimark-Sacker bifurcation are described for refuge and alternative response maps (Hong and Zhang, 2023; Chen and Li, 2024; Liu et al., 2025). Comprehensive nonlinear analysis and classification will also require the normal form and resonance conditions.

The coexistence of separate attractors at r = 4.4 represents an important case for numerical computation. Rajni and Ghosh (2022) also documented multistability in a discrete predator-prey model. Functional-response saturation and mortality affects the amplitude of the oscillations of the populations, but these deterministic trajectories can not be interpreted as survey data on natural populations. The parameter values used in the model are selected to illustrate certain phenomena of interest using numerical examples, not fitted from observational data; the model does not account for seasonal variations, age structure, demographic stochasticity, spatial variation and movement. No inferential p-values or population-level ecological effect sizes are reported.

Given the nature of the model, estimating growth and functional-response parameters from an ecological time series, and verifying whether the inferred parameters support the expected local dynamics, would be a reasonable next step. Since some phenomena in the model are coincidental and contingent on certain numerical values, which may not hold in a real biological situation, as (Jin, 2023; Ruan & Li, 2024; Zhang et al., 2024; Khan & Uddin, 2025) observe, it would also be important to evaluate stability of attractors and basins of attraction, especially in the neighborhood of r = 4.4. A sensitivity analysis to worst-case scenarios may provide more structural model predictions and insight as to which bifurcations are biologically meaningful.

6. Conclusion

A discrete exponential predator-prey map with saturated predation allows for extinction, predator-free, and interior coexistence equilibria. The explicit Jacobian and Jury analysis

locate the boundary of coexistence stability. For an illustrative, yet complete parameterization, the flip multiplier crosses -1 at r = 3.5361; computations show equilibrium dynamics for r = 3.0, with a period two orbit for r = 3.8 and positive largest Lyapunov exponents for r = 4.7. A second mortality sweep shows a transversal crossing of the unit circle consistent with a Neimark-Sacker bifurcation. The results reported in this paper reflect purely mathematical conclusions of the stated model; they should not be interpreted as an estimate of actual population levels. It is recommended that future research focuses on calculating normal form coefficients and mapping basins of attraction. Further, it is advised that parameters be adjusted in accordance to traceable ecological time series

References

Al-Basyouni, K. S., & Khan, A. Q. (2020). Discrete-time predator-prey model with bifurcations and chaos. Mathematical Problems in Engineering, 2020, Article 8845926. https://doi.org/10.1155/2020/8845926

Al-Kaff, M. O., El-Metwally, H. A., Elsadany, A.-E. A., & Elabbasy, E. M. (2024). Exploring chaos and bifurcation in a discrete prey–predator based on coupled logistic map. Scientific Reports, 14, Article 16118.

https://doi.org/10.1038/s41598-024-62439-8

Arias, C. F., Blé, G., & Falconi, M. (2022). Dynamics of a discrete-time predator–prey system with Holling II functional response. Qualitative Theory of Dynamical Systems, 21, Article 31. https://doi.org/10.1007/s12346-022-00562-5

Chen, D., & Li, X. (2024). Complex bifurcation phenomena seized in a discrete ratio-dependent Holling-Tanner predator-prey system. Advances in Continuous and Discrete Models, 2024, Article 58. https://doi.org/10.1186/s13662-024-03855-y

Hamada, M. Y., El-Azab, T., & El-Metwally, H. (2023). Bifurcations and dynamics of a discrete predator–prey model of ricker type. Journal of Applied Mathematics and Computing, 69, 113–135. https://doi.org/10.1007/s12190-022-01737-8

Hong, B., & Zhang, C. (2023). Neimark–Sacker bifurcation of a discrete-time predator–prey model with prey refuge effect. Mathematics, 11(6), Article 1399. https://doi.org/10.3390/math11061399

Khan, M. M., & Uddin, M. J. (2025). Chaos and bifurcations of a discretized Holling-II prey-predator model including prey refuge and Allee effect. Scientific Reports, 15, Article 32940. https://doi.org/10.1038/s41598-025-04333-5

Liu, M., Ma, L., & Hu, D. (2024). Some bifurcations of codimensions 1 and 2 in a discrete predator–prey model with non-linear harvesting. Mathematics, 12(18), Article 2872. https://doi.org/10.3390/math12182872

Liu, Y., Guo, L., & Liu, X. (2025). Multiple bifurcation analysis in a discrete-time predator–prey model with Holling IV response function. Symmetry, 17(9), Article 1459. https://doi.org/10.3390/sym17091459

Lv, L., & Li, X. (2024). Stability and bifurcation analysis in a discrete predator–prey system of Leslie type with radio-dependent simplified Holling type IV functional response. Mathematics, 12(12), Article 1803.

https://doi.org/10.3390/math12121803

Mehdi, R., Wu, R., & Hammouch, Z. (2025). Chaotic bifurcation dynamics in predator–prey interactions with logistic growth and Holling type-II response. Alexandria Engineering Journal, 115, 119–130.

https://doi.org/10.1016/j.aej.2024.11.077

Rajni, & Ghosh, B. (2022). Multistability, chaos and mean population density in a discrete-time predator–prey system. Chaos, Solitons & Fractals, 162, Article 112497. https://doi.org/10.1016/j.chaos.2022.112497

Ruan, M., & Li, X. (2024). Complex dynamical properties and chaos control for a discrete modified Leslie-Gower prey-predator system with Holling II functional response. Advances in Continuous and Discrete Models, 2024, Article 30. https://doi.org/10.1186/s13662-024-03828-1

Santra, P. K., Mahapatra, G. S., & Phaijoo, G. R. (2021). Bifurcation analysis and chaos control of discrete prey–predator model incorporating novel prey–refuge concept. Computational and Mathematical Methods, 3(6), e1185.

https://doi.org/10.1002/cmm4.1185

Seralan, V., Vadivel, R., Chalishajar, D., & Gunasekaran, N. (2023). Dynamical complexities and chaos control in a Ricker type predator-prey model with additive Allee effect. AIMS Mathematics, 8(10), 22896–22923. https://doi.org/10.3934/math.20231165

Singh, A., & Sharma, V. S. (2023). Bifurcations and chaos control in a discrete-time prey–predator model with Holling type-II functional response and prey refuge. Journal of Computational and Applied Mathematics, 418, Article 114666.

https://doi.org/10.1016/j.cam.2022.114666

Zhang, H., Guo, F., Zou, H., Zhao, L., Wang, Z., Yuan, X., & Liu, Z. (2024). Refuge-driven spatiotemporal chaos in a discrete predator-prey system. Chaos, Solitons & Fractals, 182, Article 114613. https://doi.org/10.1016/j.chaos.2024.114613